# Contraction tests of lead-stainless steel composites from room temperature to 77 K using strain gauges

**Summer student:** Ashley Shaw*

**Supervisor:** Fernando Aretio-Zárate

*E-mail: ashleyshaw275@gmail.com

**Abstract.** ALLEGRO is a proposed FCC-ee general-purpose detector concept with a noble-liquid electromagnetic calorimeter (ECAL) as one of its central detectors. Noble-liquid calorimetry is a strong option for future particle physics experiments – for both, hadron and lepton colliders. Such an ECAL is composed of a sandwich of 1536 multi-layer read-out electrodes realised as PCBs and the same number of absorbers immersed in a liquified noble gas at cryogenic temperatures. The absorbers are made of metallic composites using a lead core and stainless steel skin. The contraction of this material, from room temperature to 77 K, is studied by using analytical, simulation and testing techniques.

**Table of contents**

## 1. Introduction

In the design of the new detector ALLEGRO, where a noble-liquid calorimeter is one of the central detectors, an understanding of the components of the latter is required. In sampling calorimeters, one of the essential elements are the absorbers which help reach the required number of radiation lengths while keeping a compact detector and reduce the Molière radius.

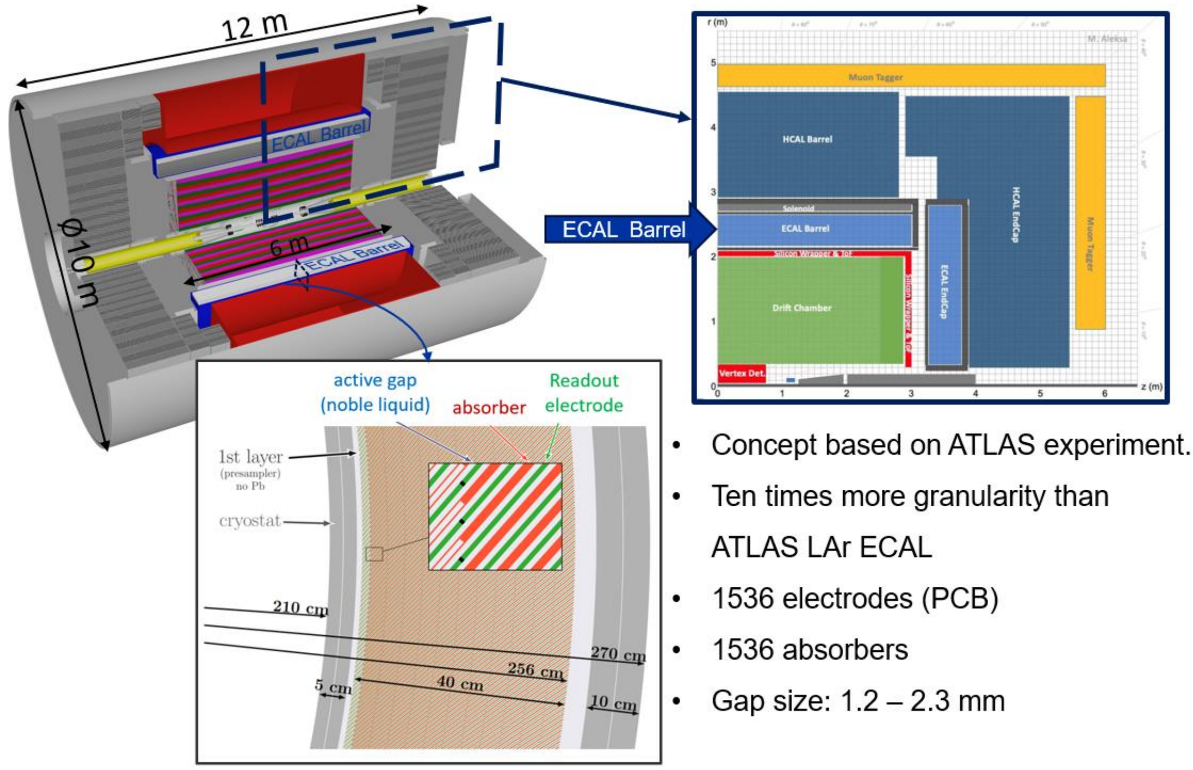


**Figure 1.** ALLEGRO full detector concept and the electromagnetic calorimeter details

In the case of the ALLEGRO ECAL, lead is the main material of the absorbers. Its low stiffness requires external layers to enhance rigidity forming a composite material. The ECAL works at cryogenic temperatures, and different coefficients of thermal expansion (CTE) induce significant additional stress with large temperature changes in sandwich materials, such as the absorbers, or structures. This effect can cause materials to plastify or even collapse. Therefore, the equivalent CTE of the absorbers' material needed to be calculated. Firstly, the laminate theory was used to analytically study the problem and have a first estimation. Secondly, several finite elements models were done, using 2D or 3D elements, to check the strains and the contraction. Finally, the calculated values were compared to experimental results, which were extracted using strain gauges.

## 2. Absorbers geometry and contraction behaviour

The plates in the absorber consist of a central 1.8mm layer of lead sandwiched between 0.05 mm of FR4 prepreg that is used to adhere an outer 0.05 mm of stainless steel. This gives a total thickness of 2 mm Figure 2. Absorber cross-section. ALLEGRO will have absorbers with the dimensions of 0.568 x 3 m but for this experiment the size was reduced to 200 x 200 mm. Additional testing and simulations were carried out with absorbers with 0.1 mm of stainless steel.


**Figure 2.** Absorber cross-section

For ease of testing, liquid nitrogen (77 K) was used instead of liquid argon (87.3 K). The absorbers start at room temperature (~300 K) and are lowered to the temperature of liquid nitrogen. Under these low temperatures, the absorbers contract.

If each of the 5 layers weren't bonded to each other, each material's coefficient of thermal expansion (CTE, symbol $\alpha$) would cause the layers to contract by different amounts **Figure 3.** Free contraction of the absorber layers. The amount that the material contracts under the temperature difference is described by the thermal strain ($\varepsilon_{thermal}$) Equation 1 . In this scenario the plates only undergo thermal strain and experience no stress. It is shown that lead contracts the most because of its high CTE.


**Figure 3.** Free contraction of the absorber layers

$$\varepsilon_{thermal} = \alpha \cdot \Delta T \qquad \text{Equation 1}$$

If the plates are assumed to be perfectly bonded, the absorber will contract a certain amount once at 77 K, this is the total strain ($\varepsilon_{total}$), resulting an equivalent length (**Figure 4**). This can be calculated using the thickness, Young´s Modulus and $\varepsilon_{thermal}$ of each layer giving a value of - 0.0046 (Equation 2).

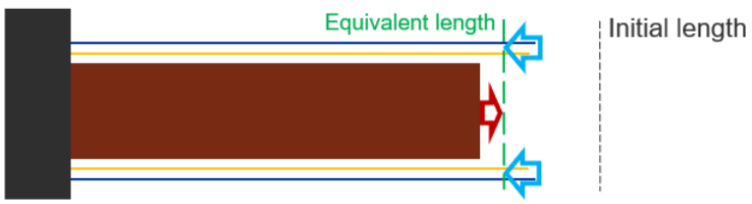


**Figure 4.** Absorber layers under compression and tension

$$\varepsilon_{total} = \frac{\Sigma(E \cdot t \cdot \varepsilon_{thermal})}{\Sigma(E \cdot t)} \qquad \text{Equation 2}$$

Mechanical strain of each layer can then be calculated from the $\varepsilon_{total}$ and $\varepsilon_{thermal}$ Equation 3.

$$\varepsilon_{total} = \varepsilon_{thermal} + \varepsilon_{mechanical} \qquad \text{Equation 3}$$

The different materials have different mechanical strain. Lead, which has the highest CTE, has a positive mechanical strain and therefore is in tension. The stainless steel and FR4 layers however are in compression. These calculations don't consider the different Poisons ratios of each layer. Using the laminate theory discussed later (section 4), a more accurate value of - 0.0048 can be found for the total strain.

| Material | Thickness (mm) | Young Modulus (GPa) | $\alpha$ ($10^{-6}$·1/K) | $\varepsilon_{thermal}$ | $\varepsilon_{mechanical}$ |
|---|---|---|---|---|---|
| 304L Stainless Steel | 0.10 | 214.8 | 13.3 | -0.0030 | -0.0016 |
| FR4 | 0.10 | 24.6 | 15.0 | -0.0033 | -0.0013 |
| Lead | 1.80 | 22.2 | 25.1 | -0.0056 | 0.0010 |
| Total / Equivalent | 2.00 | 32.0 | 20.7 | -0.0046 | n/a |

**Table 1.** Material properties and strains using proportional calculations

## 3. Contraction according to the laminate theory

Using laminate theory [1], the equivalent laminate properties were determined using material properties such as the Youngs modulus, Poisons ratio and CTE **Table 2**. Material Properties. It was expected the lead would yield, though the laminate theory is a linear analysis. Therefore, calculations were carried out with plastic and elastic lead as it was expected that the mechanical stress experienced by the lead would be enough to plastify it.

<table>
<tr><th>Material</th><th>Young Modulus (GPa)</th><th>Poison Ratio</th><th>$\alpha$ ($10^{-6}$·1/K)</th></tr>
<tr><td>304 Stainless Steel</td><td>214.80</td><td>0.290</td><td>13.3</td></tr>
<tr><td>FR4</td><td>24.60</td><td>0.136</td><td>15.0</td></tr>
<tr><td>Lead elastic</td><td>22.23</td><td rowspan="2">0.440</td><td rowspan="2">25.1</td></tr>
<tr><td>Lead plastic</td><td>0.33</td></tr>
</table>

**Table 2.** Material Properties

The results showed a lower CTE for the calculations using plastic lead, as in this case the contraction was dominated by the stainless steel which has a lower CTE ($13.3 \cdot 10^{-6}\ 1/K$). In contrast with elastic lead the CTE was more similar to that of lead ($25.1 \cdot 10^{-6}\ 1/K$). The absorber with thicker stainless steel showed a lower CTE as on average the composite had a lower CTE because of the extra stainless steel.

| SS Thickness (mm) | Stiffness of Lead (GPa) | $\alpha$ ($10^{-6}$·1/K) |
|---|---|---|
| 2x0.05 | 22.23 | 21.41 |
| 2x 0.05 | 0.33 | 13.81 |
| 2x 0.1 | 22.23 | 19.59 |
| 2x 0.1 | 0.33 | 13.57 |

**Table 3.** Laminate analysis results

## 4. Contraction according to Finite Element Analysis

Finite elements (FE) simulations were carried out using Ansys Mechanical using both a 2D layered section and 3D model. As with the laminate theory the model assumed the layers of the absorber were bonded perfectly. A thermal condition was applied to the laminate that changed the temperature from 300 K to 77 K. The plate was fixed in one corner for the 2D and 3D simulations with the latter also requiring frictionless supports on two of the adjacent faces to ensure the model was constrained **Figure 5.** 2D and 3D model constraints.

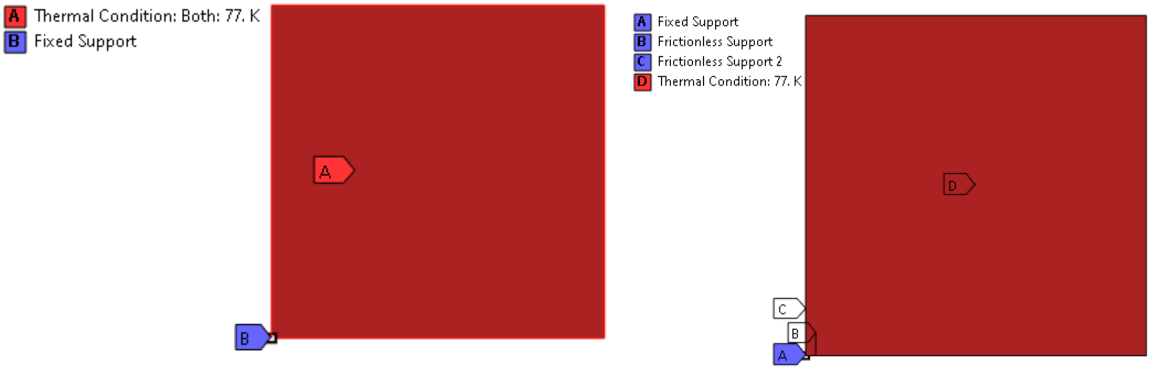


**Figure 5.** 2D and 3D model constraints

For both the 0.05 mm and 0.1 mm stainless steel plates a range of simulations were carried out in 2D using different material properties. These included elastic lead, plastic lead and bi-linear lead and stainless steel as well as simulations with a single set of materials properties at 77 K and ones where the material properties varied depending on the temperature. For the 3D simulations only bi-linear material properties that depended on the temperature were used.

Some of the key results from the simulations included the directional displacement, thermal strain and mechanical strain. Using the 2D elastic lead simulation with material properties at 77 K as an example, the total CTE of the material can be calculated using the minimum displacement (**Figure 6.** Displacements in the 2D FEM using elastic lead at 77 K) which is divided by 200 mm and then by the temperature difference (Equation 1). In this simulation, the displacement was -0.95 mm which gives a total strain of -0.004775 and a CTE of $21.41 \cdot 10^{-6}\ 1/K$.

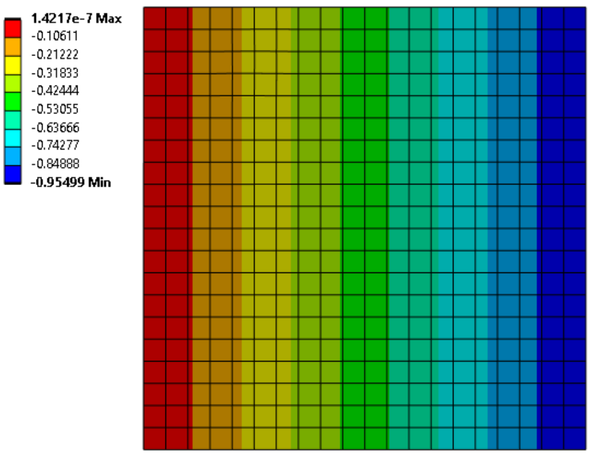


**Figure 6.** Displacements in the 2D FEM using elastic lead at 77 K

The thermal and mechanical strains for the different laminate layers was collected (**Table 4.** ), using Equation 3 these can be combined to give the total strain. The total strain of the composite was shown to be the same for both the lead and stainless steel layers as expected. This is equal to the total strain calculated previously.

| **Material** | **$\alpha$ (10$^{-6}$·1/K)** | $\varepsilon_{thermal}$ | $\varepsilon_{mechanical}$ | $\varepsilon_{total}$ |
|---|---|---|---|---|
| 304L Stainless Steel | 13.3 | -0.002967 | -0.001808 | -0.004775 |
| Lead | 25.1 | -0.005597 | 0.000822 | -0.004775 |

**Table 4.** Strains in the 2D FEM using elastic lead at 77 K

The results showed that the simulations that used elastic lead had the highest deformation and thus CTE. Those using plastic lead had the lowest deformation. The bi-linear simulations considered the material's reduced Young modulus after the yield point was reached and had deformations slightly higher than plastic lead. The values for the CTE of the absorber was lower for the simulations that used 0.01 mm stainless steel.

The 2D simulations that had material properties that varied with temperature showed very similar results to those that only used the properties for 77 K. The 3D simulations that used bi-linear material propertied that varied with temperature showed results close to those of the 2D bi-linear simulations.

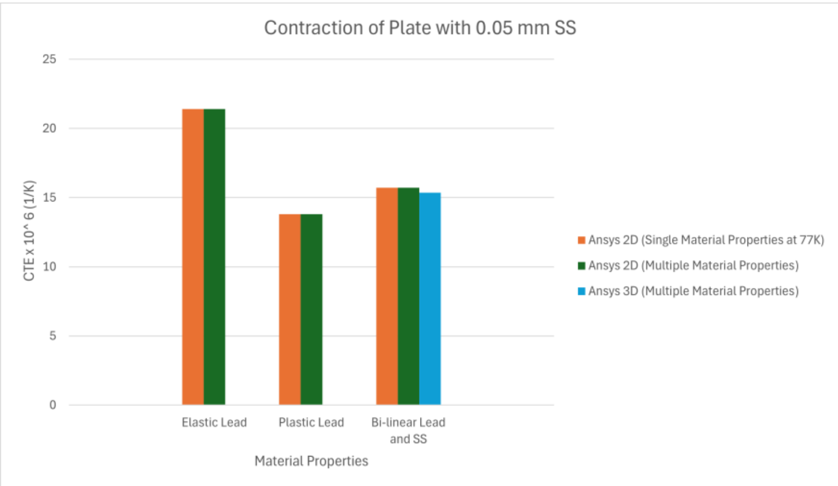


**Figure 7.** CTE for 0.05 mm stainless steel

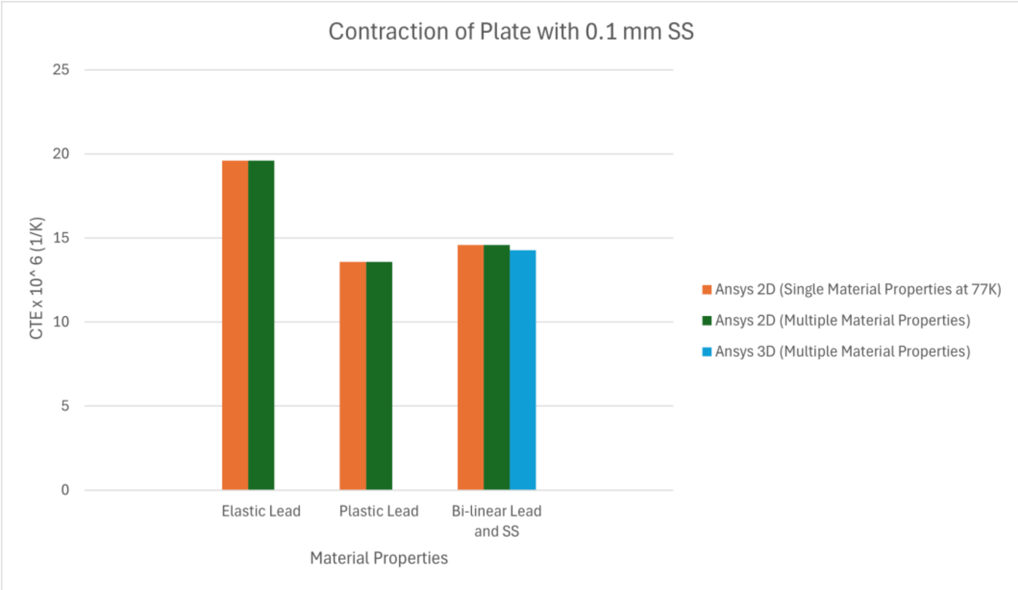


**Figure 8.** CTE for 0.1 mm stainless steel

## 5. Test

### *5.1. Set-up*

A strain gauge was epoxied to the centre of both the 0.05 mm and 0.1 mm thick stainless steel plates using EA-2A. A temperature sensor was taped adjacent to the strain gauge **Figure 9**. Experiment setup. Previous testing compared the EA-2A epoxy (which was recommended by the strain gauge manufacturer) to Stycast 1266 A (with CAT 24 LV) and CMR Direct GE Varnish. The GE Varnish failed to adhere the strain gauge to the stainless steel test piece after being submerged in liquid nitrogen. EA-2A was chosen.

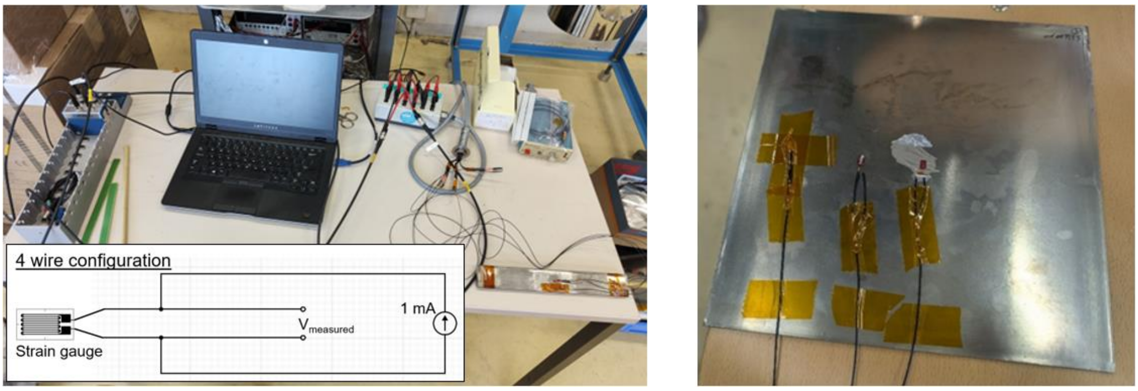


**Figure 9.** Experiment setup and *4 wire configuration* sketch

The strain gauge and temperature sensor were supplied separately with 1 mA from a current source using a four wire configuration. The resistance of the strain gauge changed depending on the strain with a nominal value of 350 Ω. This was calculated by dividing the voltage of the strain gauge measured using a DAC by the 1 mA current. The strain was calculated using the change in resistance and the gauge factor (k = 2.09) of the strain gauges (Equation 4). $R_0$ is calculated by taking the voltage at the beginning of the test, at room temperature.

$$\varepsilon = \frac{\frac{R - R_0}{R_0}}{k} \qquad \text{Equation 4}$$

The absorber plates were submerged in the liquid nitrogen whilst suspended from a chain for approximately 2 minutes (**Figure 10**). Next, the absorbers were allowed to warm until they had returned to their original size. The same test was carried out with a reference material that had a known CTE, in this case a bar of stainless steel.

**Figure 10.** Absorber suspended from chain during the cold down (left) and the warming up (right)

*5.2. Results*

The coefficient of thermal expansion of the two plates was calculated by subtracting the strain observed on the surface of the plate ($\varepsilon_m$) by that of the stainless steel reference material ($\varepsilon_r$). This was then divided by the temperature difference and added to the CTE of the reference material Equation 5. The results were calculated for both 0.05 mm and 0.1 mm stainless steel (**Table 5.** Test results).

$$\alpha = \frac{\varepsilon_m - \varepsilon_r}{\Delta T} + \alpha_r \qquad \text{Equation 5}$$

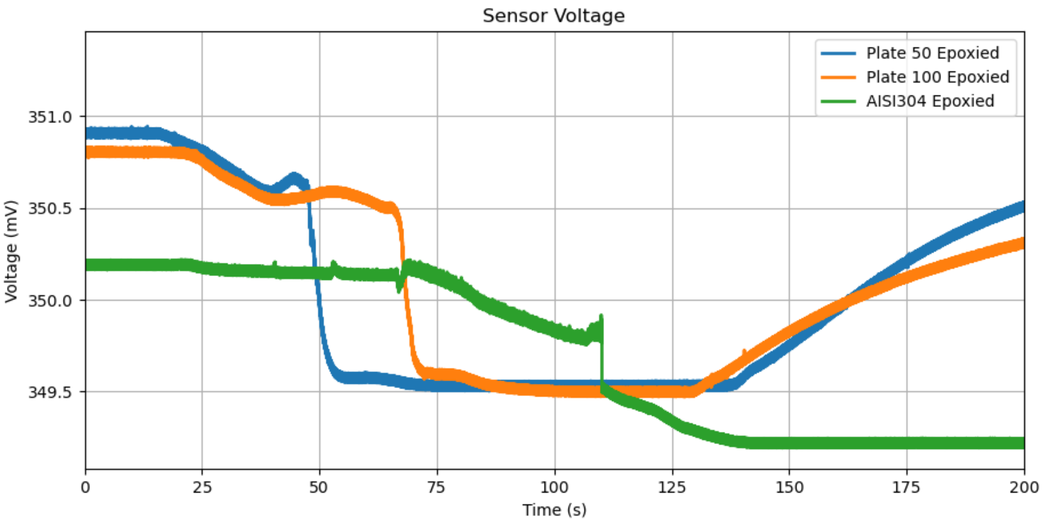


**Figure 11.** Measured strain gauge voltages

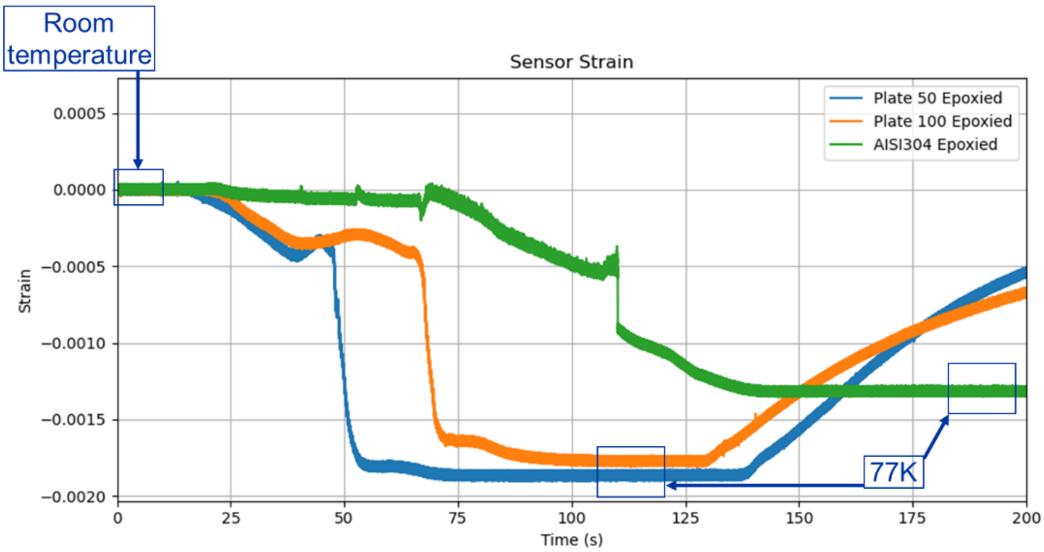


**Figure 12.** Adjusted strain gauge values

| Plate | εm | εr | CTE ref [1/K] | CTE mat [1/K] |
|---|---|---|---|---|
| 2x0.05 mm | -0.001880 | -0.001329 | $13.30 \cdot 10^{-6}$ | $15.76 \cdot 10^{-6}$ |
| 2x0.10 mm | -0.001780 | -0.001329 | $13.30 \cdot 10^{-6}$ | $15.33 \cdot 10^{-6}$ |

**Table 5.** Test results

*5.3. Discussion*

The calculated CTE fits the results of another experiment, where displacement sensors were used. In that case, using stainless steel sheets of 0.05 mm, the CTE was on average $15.6 \cdot 10^{-6}$ 1/K. Taking into account the standard deviation of the test, shown in Figure 14, the results obtained by the strain gauges seemed consistent.

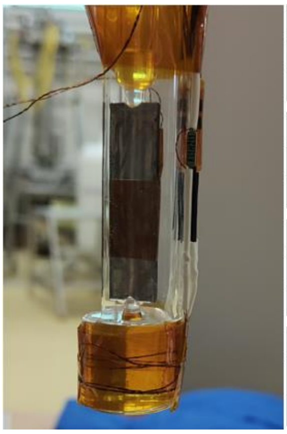

| Lead-SS sample 1 | Test 1 | Test 2 | Test 3 |
|---|---|---|---|
| Between 273K and 77K | 3.31E-03 | 3.26E-03 | 3.33E-03 |
| Between RT and 77K | 3.48E-03 | 3.57E-03 | 3.66E-03 |

| Lead-SS sample 2 | Test 1 | Test 2 | Test 3 |
|---|---|---|---|
| Between 273K and 77K | 3.55E-03 | 3.41E-03 | 3.55E-03 |
| Between RT and 77K | 3.65E-03 | 3.65E-03 | 3.82E-03 |

| Lead-SS sample 3 | Test 1 | Test 2 | Test 3 | Test 4 |
|---|---|---|---|---|
| Between 273K and 77K | 2.98E-03 | 3.10E-03 | 2.98E-03 | 3.21E-03 |
| Between RT and 77K | 3.13E-03 | 3.29E-03 | 3.29E-03 | 3.31E-03 |

| Lead-SS Average | Average | Std Dev | CTE [1/K] |
|---|---|---|---|
| Between 273K and 77K | 3.27E-03 | 6.32% | 1.67E-05 |
| Between RT and 77K | 3.49E-03 | 6.28% | 1.56E-05 |

**Figure 13.** Strain and CTE values of the sensor displacement test

The test produced CTE values that were lower for the absorber with thicker stainless steel. This was likely due to the average CTE of the material being lower because of the extra stainless steel especially after the lead plasticised.

## 6. Conclusions

After the contraction of the absorber was tested with the liquid nitrogen, the strain and CTE was calculated. Comparisons were made between laminate theory analysis and 2D and 3D Ansys simulations. The results were consistent between the different methods at predicting the contraction behaviour. The results that were the most accurate included bi-linear material properties that started elastic and then experienced a reduced Young's modulus after yielding. The thermal contraction was less with the absorber that included thicker layers of stainless steel (0.1 mm thick) as once the lead had yielded the extra stainless steel and its lower CTE had a bigger impact on reducing the overall CTE.

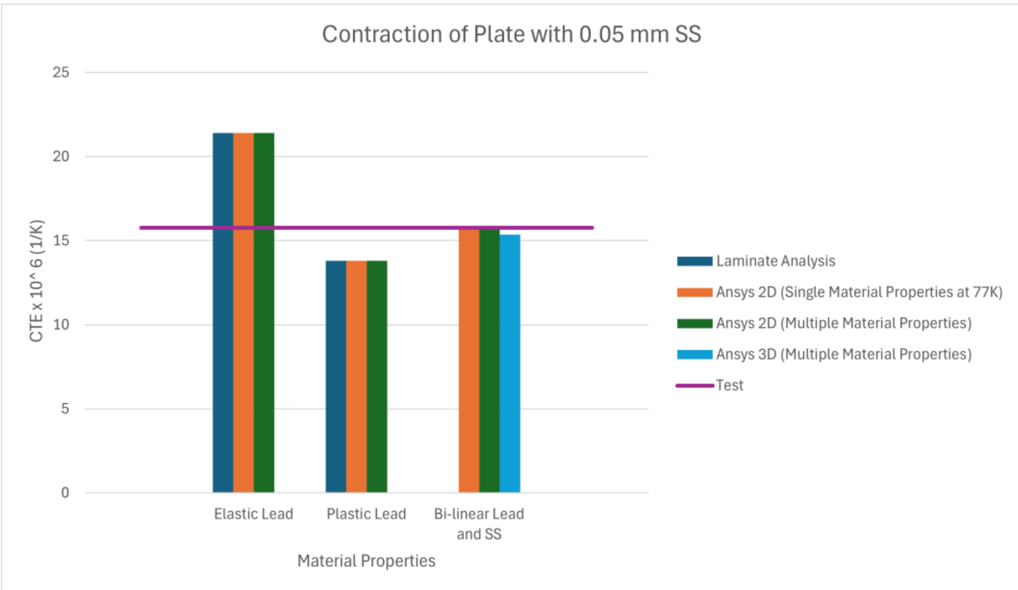


**Figure 14.** Comparison of results for 0.05 mm steel

The test results showed CTE values that closely matched the simulations that used bi-linear material properties (Figure 14). All methods of simulation showed similar results to the laminate theory, though the bi-linear material case wasn't possible with the laminate analysis. The fact that the results matched the plasticised lead more than the plastic lead show that the lead yielded early meaning it had a lower effect on the overall CTE (reducing the CTE). The plastic phase still had an effect as the bi-linear results showed slightly higher contraction that the purely plastic case.

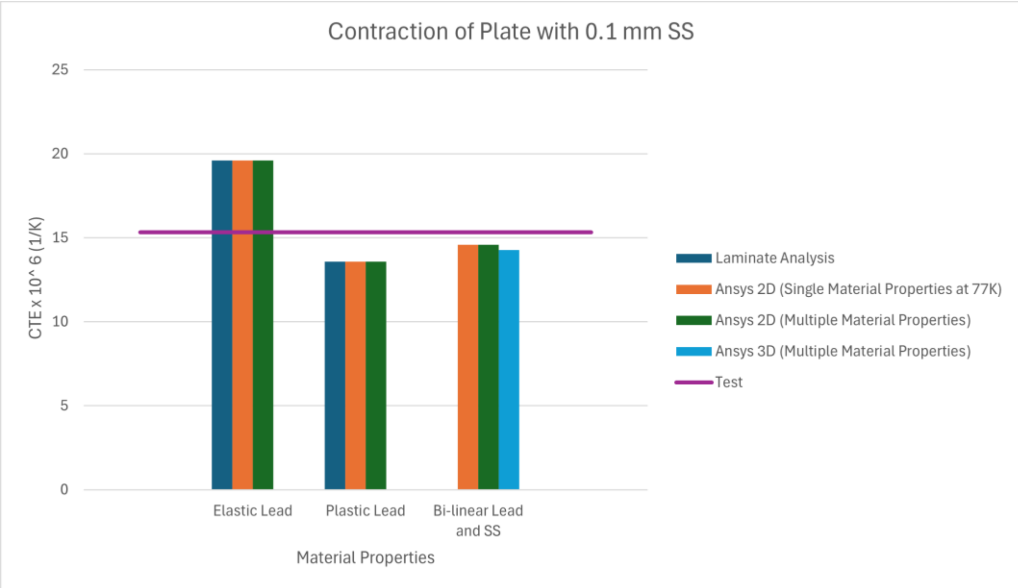


**Figure 15.** Comparison of results for 0.1 mm steel

## 7. References


[1] A.T.Nettles, "Basic Mechanics of Laminated Composite Plates," NASA, 1994.